Characteristic Model-based Station-keeping Control for Halo Orbits about Sun-Earth L1 Point

Bin Zhang
Beijing Institute of Control Engineering
China Academy of Space Technology
Beijing, China
buaa_zbin13@163.com

Jing Zhou
Beijing Institute of Control Engineering
China Academy of Space Technology
Beijing, China
zhoujing_bice@126.com

***Abstract*—Halo orbits about libration points are believed to be useful in future deep-space missions. In this work, a station-keeping strategy based on characteristic model theory is proposed within the elliptic restricted three-body problem. A golden-section controller for velocity tracking and a PD controller for position tracking are designed respectively for the station-keeping control of halo orbit about the L1 point of the Sun-Earth system. The simulation shows that this strategy can reach a relatively high precision in station-keeping control, where the tracking errors are no more than 2508.8 m in position and 0.251 m/s in velocity. The velocity increment required during the stable stage is only 3.7873 m/s per period.**

Keywords—libration points, halo orbit, ERTBP, station-keeping control, characteristic model, golden-section controller, PD controller

I. INTRODUCTION

It is well known that there are five equilibrium points in the restricted three-body problem(RTBP), which are called libration points. Particularly, the three that locate on the line joining the two primaries are called collinear libration points[1]. These libration points have some good properties and are believed to potentially play an essential role in future deep space explorations. Firstly, there are various types of orbits about libration points, including periodic halo orbits and Lissajous orbits et al. [2], which provides a wide range of choices for different aims; secondly, according to the dynamics of three-body problem, when a satellite is located on a libration point, its relative position to the primaries will remain unchanged forever; thirdly, the locations of libration points in space will potentially bring advantages to particular missions, for example, Sun-Earth L_1 point is an ideal location for observation of Sun's activities[3], whereas orbits around Earth-Moon L_2 point can serve as the mission orbit for satellites aiming at establishing a communication link between Earth and the far side of Moon[4]. During the past four decades, several missions using libration point orbits have been successfully launched, such as ISEE-3, SOHO, Genesis and Queqiao et al. [5]. All of these missions have gotten plenty of outcomes and proved the value of libration point orbits, especially halo orbits.

Due to the instability of collinear libration points, orbits around them are unstable. In real mission, satellites, if not controlled, will deviate from the target libration point orbits rapidly. So maintenance control is necessary. Many researchers have been working on this problem, and different strategies have been developed. Howell and Pernicka[6] proposed a target shooting strategy for station-keeping control of halo orbits around Earth-Moon collinear libration points and applied it successfully to ARTEMIS mission. A H_∞ optimal control strategy for halo orbits was proposed by Kulkami[7] and simulation was done under Sun-Earth L_1 point circumstance. Xu[8] designed a robust adaptive strategy and applied it to the stationkeeping of halo orbit around Sun-Earth L_1 point as well. What's more, three different strategies, which are time-varying LQR control, backstepping strategy, and feedback linearization, were studied by Nazari[9]. A comparison between the simulation results of those strategies showed that the backstepping strategy required the lowest controlling consumption.

In this work, we studied the station-keeping control of halo orbits in the Sun-Earth system using a strategy based on the characteristic model. The characteristic model theory was first proposed by Wu Hong-xin in the 1980s. According to [10], characteristic model is constructed based on the object's original dynamics but has a simplified form and an equivalent output if given the same input, thus making the design of controller easier to be done. Since the three-body problem is more complicated than two-body problem and has more complicated dynamics, using the characteristic model theory to obtain a simplified but equivalent dynamic will surely bring some advantages. In sections II, we firstly introduce the dynamics involved and calculate the reference trajectory; in section III, a golden-section controller and a PD controller are designed based on characteristic model; in section IV, we will give the simulation results of halo orbits around Sun-Earth L_1 point; in the final section, we will conclude our work and give the conclusion.

II. DYNAMICAL MODEL AND REFERENCE TRAJECTORY

A. Circular Restricted Three-Body Problem

Circular restricted three-body problem(CRTBP) is an ideal simplification of RTBP. It describes the motion of a particle with a very small mass under the gravity of two massive primaries that are in circular motion around the common center of masses[1]. In this work, we choose Sun and Earth-Moon barycenter as two primaries, satellite as the particle.

For the convenience of calculation, the CTRBP is usually studied under syzygy frame with normalized units of mass, length and time as follow:

$$\begin{aligned} &[M] = M_1 + M_2 \\ &[L] = L_{12} \\ &[T] = \left[\frac{L_{12}^3}{G(M_1 + M_2)} \right]^{\frac{1}{2}} \end{aligned} \tag{1}$$

where M_1 and M_2 denote the masses of Sun and Earth-Moon respectively, L_{12} denotes the average distance between Sun and Earth-Moon barycenter, G denotes the universal gravitational constant.

The syzygy frame is shown in Fig.1, where m_3 denotes the satellite; M_1 and M_2 denote the primaries. The origin O locates at the mass center of the system, Ox points from M_1 to M_2 ; Oz has the same direction with the angular momentum of the motion of M_1 and M_2 . $\boldsymbol{r}$, $\boldsymbol{r}_1$ and $\boldsymbol{r}_2$ are the vectors from O , M_1 and M_2 to m_3 .

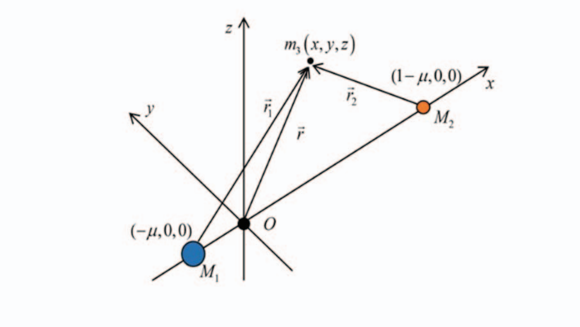

Fig. 1 Syzygy frame

Let $\mu = M_2/[M]$, then we can get the normalized positions of primaries in the syzygy frame, which are $(-\mu,0,0)$ and $(1-\mu,0,0)$ respectively. In Sun-Earth/Moon system, $\mu = 3.04036\times10^{-6}$.

Let $[x \quad y \quad z]^T$ denotes the coordinate of m_3 in syzygy frame, the equations of motion can be formulated as follow:

$$\begin{cases} \ddot{x} - 2\dot{y} = \dfrac{\partial \Omega}{\partial x} \\ \ddot{y} + 2\dot{x} = \dfrac{\partial \Omega}{\partial y} \\ \ddot{z} = \dfrac{\partial \Omega}{\partial z} \end{cases} \tag{2}$$

where

$$\begin{aligned} \Omega &= \frac{1}{2}\left(x^2+y^2\right) + \frac{1-\mu}{r_1} + \frac{\mu}{r_2} \\ r_1 &= \left[\left(x+\mu\right)^2 + y^2 + z^2\right]^{\frac{1}{2}} \\ r_2 &= \left[\left(1-x-\mu\right)^2 + y^2 + z^2\right]^{\frac{1}{2}} \end{aligned} \tag{3}$$

B. *Elliptic Restricted Three-Body Problem*

In the CRTBP model, the eccentricity of the orbit of Earth and other perturbations was ignored, which is precise enough for analysis under ideal circumstances, but not enough for real task. Taking the eccentricity into account, we can get a more precise model, which is called the elliptic restricted three-body problem(ERTBP). In ERTBP, the definitions of coordinate axis are the same as CRTBP, but the orbit of the small primary complies with the two-body Keplerian motion.

According to [11] and [12], considering the effect of solar radiation, the equations of motion can be formulated as follow:

$$\begin{cases} \ddot{x} - 2\dot{y} = \dfrac{\partial W}{\partial x} + \tilde{K}\tilde{S}\dfrac{(x+\mu)}{r_1^3} \\ \ddot{y} + 2\dot{x} = \dfrac{\partial W}{\partial y} + \tilde{K}\tilde{S}\dfrac{y}{r_1^3} \\ \ddot{z} = \dfrac{\partial W}{\partial z} + \tilde{K}\tilde{S}\dfrac{z}{r_1^3} \end{cases} \tag{4}$$

where $[x \quad y \quad z]^T$ denotes the coordinate of m_3 ; W has the form as follow:

$$W = \frac{1}{1+e\cos f}\left(\frac{\left(x^2+y^2\right)}{2} - \frac{ez^2\cos f}{2} + \frac{1-\mu}{r_1} + \frac{\mu}{r_2}\right) \tag{5}$$

where e denotes the eccentricity; f denotes the true anomaly of the small primary.

$\tilde{K}$ denotes the coefficient of reflectivity with a value between 0 and 2. $\tilde{S}$ denotes the solar flux calculated through

$$\tilde{S} = \frac{\tilde{A}\tilde{S}_0 r_0^2}{cm_3} \tag{6}$$

where $\tilde{A}$ and m_3 denote the cross-section area and the mass of the satellite respectively; $\tilde{S}_0$ denotes the solar flux over a unit area; c denotes the speed of light and r_0 is equal to 1 AU.

C. *Reference Trajectory*

A reference trajectory is the prerequisite for station-keeping control. In this work, we choose a halo orbit about Sun-Earth/Moon L_1 point as the reference trajectory. Due to the nonlinear property of the dynamics of the three-body problem, the precise analytic solution of halo orbit cannot be obtained directly. It's generally calculated through numerical integration of the dynamics.

Richardson[13] derived a three order approximate analytic solution of halo orbits through Lindstedt-Poincare method, which is shown as follow:

$$\begin{cases} x = a_{21}A_x^2 + a_{22}A_z^2 - A_x\cos\tau_1 + \left(a_{23}A_x^2 - \right. \\ \qquad \left. a_{24}A_z^2\right)\cos 2\tau_1 + \left(a_{31}A_x^3 - a_{32}A_xA_z^2\right)\cos 3\tau_1 \\ y = kA_x\sin\tau_1 + \left(b_{21}A_x^2 - b_{22}A_z^2\right)\sin 2\tau_1 + \\ \qquad \left(b_{31}A_x^3 - b_{32}A_xA_z^2\right)\sin 3\tau_1 \\ z = \delta_n\left[A_z\cos\tau_1 + d_{21}A_xA_z\left(\cos 2\tau_1 - 3\right) + \right. \\ \qquad \left. \left(d_{32}A_zA_x^2 - d_{31}A_z^3\right)\cos 3\tau_1\right] \end{cases} \tag{7}$$

where A_x and A_z denote the linearized amplitudes of halo orbit. The meanings of other parameters can be seen in [13].

Through (7), we can obtain the approximation of the initial value for numerical integration. To obtain a precise reference orbit of a years-long duration, we need firstly modify the approximate initial value by a differential correction strategy. Considering that halo orbit is symmetrical with respect to the xOz plane in syzygy frame, we select the approximate initial value as

$$X_0 = \begin{bmatrix} x_0 & 0 & z_0 & 0 & \dot{y}_0 & 0 \end{bmatrix}^T$$

then fix z_0 and adjust the value of x_0 and $\dot{y}_0$ to make the final value of $\dot{x}_d$ and $\dot{z}_d$ close to zero gradually. The corrections can be obtained through the following equations:

$$\begin{bmatrix} \delta\dot{x}_d \\ \delta\dot{z}_d \end{bmatrix} = \left(\begin{bmatrix} \Phi_{41} & \Phi_{45} \\ \Phi_{61} & \Phi_{65} \end{bmatrix} - \frac{1}{\dot{y}_0} \begin{bmatrix} \ddot{x}_d \\ \ddot{z}_d \end{bmatrix} \begin{bmatrix} \Phi_{21} & \Phi_{25} \end{bmatrix} \right) \begin{bmatrix} \delta x_0 \\ \delta y_0 \end{bmatrix}$$

the meanings of the parameters can be seen in [14]. With the aforementioned strategy, we can obtain the modified initial value for numerical integration.

However, the modified initial value is still not precise enough to obtain a long term reference orbit. If we integrate the dynamics with the modified initial value, the orbit will diverge within 2 period. Therefore, we use the first period of the integration as the baseline and employ the target shooting strategy to modify the reference halo orbit. The basic concept of target shooting is to minimize the following function:

$$J = \Delta v^T Q \Delta v + \sum_{k=1}^{n} \left(p_k^T R_k p_k + v_k^T T_k v_k \right) \tag{8}$$

to get a minimal $\Delta v_{\min}$ for the modification of the halo orbit. In (8), Q, R_k and T_k are weight matrixes; p_k and v_k are the position and velocity errors of the satellite in the kth target, which are obtained through the following equations:

$$\begin{aligned} \begin{bmatrix} p_k \\ v_k \end{bmatrix} &= \Phi(t_k, t_c) \begin{bmatrix} p_c \\ v_c + \Delta v \end{bmatrix} \\ &= \begin{bmatrix} A_{ic} & B_{ic} \\ C_{ic} & D_{ic} \end{bmatrix} \begin{bmatrix} p_c \\ v_c + \Delta v \end{bmatrix} \end{aligned} \tag{9}$$

The meanings of the parameters can be seen in [12]. Substitute p_k and v_k into (8) and let

$$\frac{\partial J}{\partial \Delta v} = 0 \tag{10}$$

then we can get $\Delta v_{\min}$.

Set $A_z = 0.000735$ and employ the aforementioned strategies, we can obtain a 2.5 years-long reference halo orbit shown in Fig. 2.

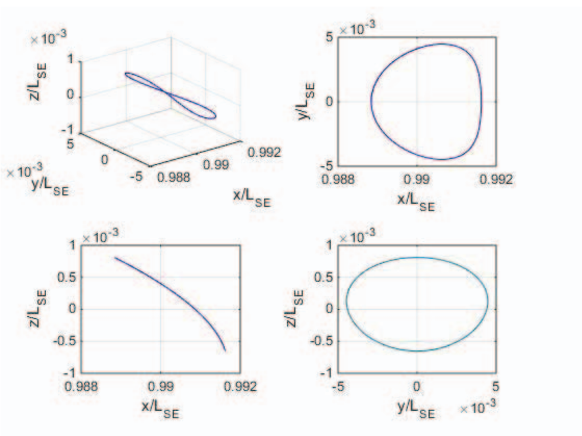

Fig. 2 Modified reference halo orbit

III. Designing of the Controller

Let $\boldsymbol{X} = \begin{bmatrix} x & y & z & \dot{x} & \dot{y} & \dot{z} \end{bmatrix}^T$, then (4) can be transformed into the following controlled form:

$$\dot{\boldsymbol{X}} = F(\boldsymbol{X}) + \boldsymbol{B}\boldsymbol{u} \tag{11}$$

where

$$F(\boldsymbol{X}) = \begin{bmatrix} \dot{x} \\ \dot{y} \\ \dot{z} \\ 2\dot{y} + \dfrac{\partial W}{\partial x} + \tilde{K}\tilde{S}\dfrac{(x+\mu)}{r_1^3} \\ -2\dot{x} + \dfrac{\partial W}{\partial y} + \tilde{K}\tilde{S}\dfrac{y}{r_1^3} \\ \dfrac{\partial W}{\partial z} + \tilde{K}\tilde{S}\dfrac{z}{r_1^3} \end{bmatrix}$$

$$\boldsymbol{u} = \begin{bmatrix} u_1 & u_2 & u_3 \end{bmatrix}^T$$

$$\boldsymbol{B} = \begin{bmatrix} \boldsymbol{0}_{3\times3} & \boldsymbol{I}_{3\times3} \end{bmatrix}^T$$

$\boldsymbol{u}$ is called the control acceleration.

A. Golden-section Controller for Velocity Tracking

Apparently, (11) is a MIMO system with three inputs and six outputs. However, according to [10], the construction of a characteristic model for a MIMO system requests the number of inputs to be equal to that of outputs, which means we can't directly construct the characteristic model for full state. Therefore, we first construct the characteristic model for velocity tracking in this work.

When the sampling period Δt fulfill some specific conditions, the characteristic model for velocity tracking can be depicted as the following output-decoupled two-order difference equations:

$$\begin{aligned} \boldsymbol{X}_1(k+1) = \boldsymbol{F}_1(k)\boldsymbol{X}_1(k) + \boldsymbol{F}_2(k)\boldsymbol{X}_1(k-1) + \\ \boldsymbol{G}_0(k)\boldsymbol{U}_1(k) + \boldsymbol{G}_1(k)\boldsymbol{U}_1(k-1) \end{aligned} \tag{12}$$

where

$$\boldsymbol{X}_1(k) = \begin{bmatrix} x_1(k) & x_2(k) & x_3(k) \end{bmatrix}^T$$

$$\boldsymbol{U}_1(k) = \begin{bmatrix} u_{11}(k) & u_{12}(k) & u_{13}(k) \end{bmatrix}^T$$

$$\boldsymbol{F}_1(k) = \begin{bmatrix} f_{11}(k) & 0 & 0 \\ 0 & f_{12}(k) & 0 \\ 0 & 0 & f_{13}(k) \end{bmatrix}$$

$$\boldsymbol{F}_2(k) = \begin{bmatrix} f_{21}(k) & 0 & 0 \\ 0 & f_{22}(k) & 0 \\ 0 & 0 & f_{23}(k) \end{bmatrix}$$

$$\boldsymbol{G}_0(k) = \begin{bmatrix} g_{0,11}(k) & g_{0,12}(k) & g_{0,13}(k) \\ g_{0,21}(k) & g_{0,22}(k) & g_{0,23}(k) \\ g_{0,31}(k) & g_{0,32}(k) & g_{0,33}(k) \end{bmatrix}$$

$$\boldsymbol{G}_1(k) = \begin{bmatrix} g_{1,11}(k) & g_{1,12}(k) & g_{1,13}(k) \\ g_{1,21}(k) & g_{1,22}(k) & g_{1,23}(k) \\ g_{1,31}(k) & g_{1,32}(k) & g_{1,33}(k) \end{bmatrix}$$

In (12), characteristic parameters, including $\boldsymbol{F}_1(k)$, $\boldsymbol{F}_2(k)$, $\boldsymbol{G}_0(k)$ and $\boldsymbol{G}_1(k)$, are obtained through parameter recognition. Each loop of (12) can be written as follow:

$$\begin{aligned} x_j(k) &= f_{1j}(k)x_j(k-1)+f_{2j}(k)x_j(k-2)+ \\ &\quad \sum_{h=1}^{3} g_{0,jh}(k)u_{1h}(k-1)+ \\ &\quad \sum_{h=1}^{3} g_{1,jh}(k)u_{1h}(k-2) \\ &= \boldsymbol{\phi}_j^T(k-1)\hat{\boldsymbol{\theta}}_j(k) \end{aligned} \tag{13}$$

where

$$\begin{aligned} \boldsymbol{\phi}_j(k-1) = \big[& x_j(k-1) \quad x_j(k-2) \quad u_{11}(k-1) \quad u_{12}(k-1) \\ & u_{13}(k-1) \quad u_{11}(k-2) \quad u_{12}(k-2) \quad u_{13}(k-2) \big]^T \\ \hat{\boldsymbol{\theta}}_j(k) = \big[& \hat{f}_{1j}(k) \quad \hat{f}_{2j}(k) \quad \hat{g}_{0,j1}(k) \quad \hat{g}_{0,j2}(k) \\ & \hat{g}_{0,j3}(k) \quad \hat{g}_{1,j1}(k) \quad \hat{g}_{1,j2}(k) \quad \hat{g}_{1,j3}(k) \big]^T \end{aligned}$$

Then, parameter recognition can be employed through the following least-squares method:

$$\begin{cases} \boldsymbol{k}_j(k) = \dfrac{\boldsymbol{p}_j(k-1)\boldsymbol{\phi}_j(k-1)}{\lambda+\boldsymbol{\phi}_j^T(k-1)\boldsymbol{p}_j(k-1)\boldsymbol{\phi}_j(k-1)} \\ \hat{\boldsymbol{\theta}}_j(k) = \hat{\boldsymbol{\theta}}_j(k-1)+ \\ \qquad \boldsymbol{k}_j(k)\left[x_j(k)-\boldsymbol{\phi}_j^T(k-1)\hat{\boldsymbol{\theta}}_j(k-1)\right] \\ \boldsymbol{p}_j(k) = \dfrac{1}{\lambda}\left[\boldsymbol{I}-\boldsymbol{k}_j(k)\boldsymbol{\phi}_j^T(k-1)\right]\boldsymbol{p}_j(k-1) \end{cases} \tag{14}$$

Based on the characteristic model shown in (12), we can design the golden-section controller as follow:

$$\begin{aligned} \boldsymbol{U}_1(k) = -\left[\hat{\boldsymbol{G}}_0(k)+\boldsymbol{\Lambda}\right]^{-1}\Big[& l_1\hat{\boldsymbol{F}}_1(k)\tilde{\boldsymbol{Y}}_1(k)+ \\ & l_2\hat{\boldsymbol{F}}_2(k)\tilde{\boldsymbol{Y}}_1(k-1)+\hat{\boldsymbol{G}}_1(k)\boldsymbol{U}_1(k-1)\Big] \end{aligned} \tag{15}$$

where $\boldsymbol{X}_1^r(k)$ is the expected output; $\boldsymbol{X}_1(k)$ is the real output and $\tilde{\boldsymbol{Y}}_1(k)=\boldsymbol{X}_1^r(k)-\boldsymbol{X}_1(k)$; $\hat{\boldsymbol{F}}_1(k)$, $\hat{\boldsymbol{F}}_2(k)$, $\hat{\boldsymbol{G}}_0(k)$ and $\hat{\boldsymbol{G}}_1(k)$ are the parameter estimations; $l_1=0.382$, $l_2=0.618$ are the golden-section numbers; $\boldsymbol{\Lambda}=diag(\lambda_1,\lambda_2,\lambda_3)$ is a positive constant matrix.

B. PD Controller for Position Tracking

In the designing of the golden-section controller, we only took the velocity errors into account, but to fulfill a full-state control, we still need to get the position errors involved. Therefore, we designed the following PD controller for position tracking:

$$\boldsymbol{u}_2 = \boldsymbol{u}_p + \boldsymbol{u}_d \tag{16}$$

In (16),

$$\boldsymbol{u}_p = \boldsymbol{K}_p\tilde{\boldsymbol{Y}}_2(k) \tag{17}$$

where $\tilde{\boldsymbol{Y}}_2(k)=\boldsymbol{X}_2^r-\boldsymbol{X}_2$ and $\boldsymbol{K}_p=diag(k_{p1},k_{p2},k_{p3})$ is a constant matrix. $\boldsymbol{X}_2^r$ is the expected output and $\boldsymbol{X}_2$ is the real output.

$\boldsymbol{u}_d$ is a logical differentiation with the following form:

$$\begin{aligned} & u_{dj} = c_j\left[x_{2j}(k)-x_{2j}(k-1)\right]\bullet \\ & \sqrt{\sum_{i=1}^{N_j}\left\{\left[\tilde{y}_{2j}(k-i)\right]^2+\left[\tilde{y}_{2j}(k-i)-\tilde{y}_{2j}(k-i-1)\right]^2\right\}} \\ & \boldsymbol{u}_d = diag(u_{d1},u_{d2},u_{d3}) \end{aligned} \tag{18}$$

where c_j and N_j are constants.

Finally, we get the controller for the station-keeping control of halo orbit:

$$\boldsymbol{u} = \boldsymbol{u}_1 + \boldsymbol{u}_2 \tag{19}$$

IV. Simulation Results

To verify the validity of the controller (19), we employed a simulation under the ERTBP model. The reference halo orbit we chose is the one shown in Fig.2, which locates at the L_1 point of the Sun-Earth system and has an amplitude of $A_z=0.000735$ equal to 110000 km. The period of the orbit is $T=3.0597$ in normalized units, which is equal to 176.7829 days. And the total simulation duration is 5 periods, which is about 2.5 years.

Considering the inevitable orbit injection errors in real mission, we add an initial error to the initial value at the beginning of the simulation, which is:

$$\Delta X_0 = \left[1000km \quad 1000km \quad 1000km\right]^T$$

$$\Delta V_0 = \left[1m/s \quad 1m/s \quad 1m/s\right]^T$$

The parameters of solar radiation we set are as follow:

$$\tilde{K}=0.6,\ \tilde{A}=3.5m^2,\ m_3=500kg$$

$$\tilde{S}_0=1358W/m^2,\ c=3\times10^8 m/s$$

The sample period of the simulation is $\Delta t=0.001$. The simulation result is shown in Fig.3.

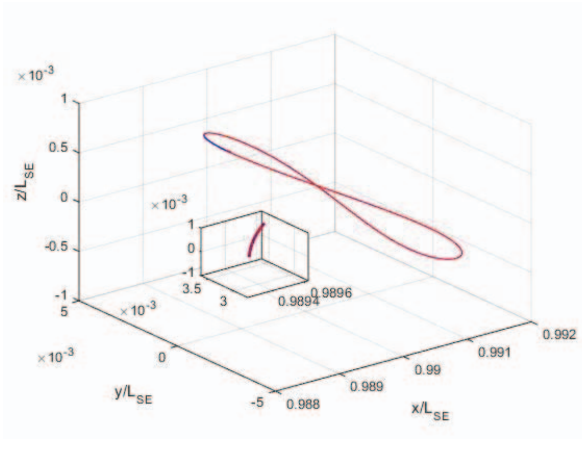

Fig. 3 Station-keeping under ERTBP model

The position errors, velocity errors, and control accelerations are shown in Fig. 4, Fig. 5 and Fig. 6. Through the error graphs, we can see that the position errors and velocity errors decline to zero rapidly. At the stable stage, the average position errors are $699.3m$, $2508.8m$ and $133.8m$; the average velocity errors are $0.0031m/s$, $0.0251m/s$ and $0.0007m/s$.

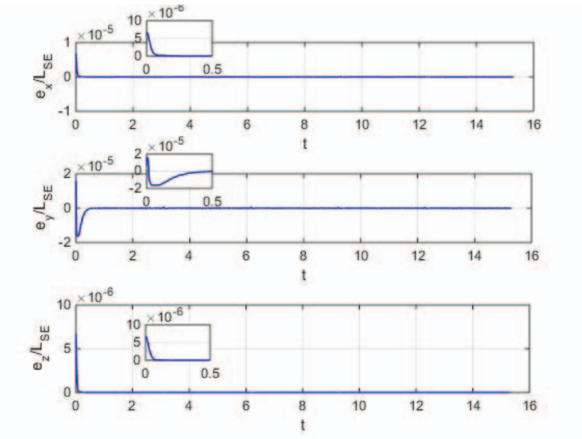

Fig. 4 Position errors

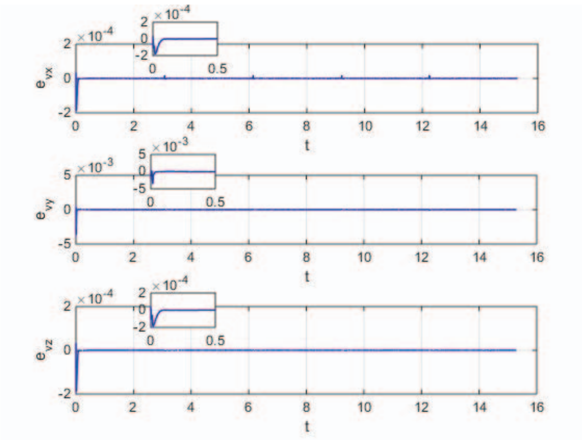

Fig. 5 Velocity errors

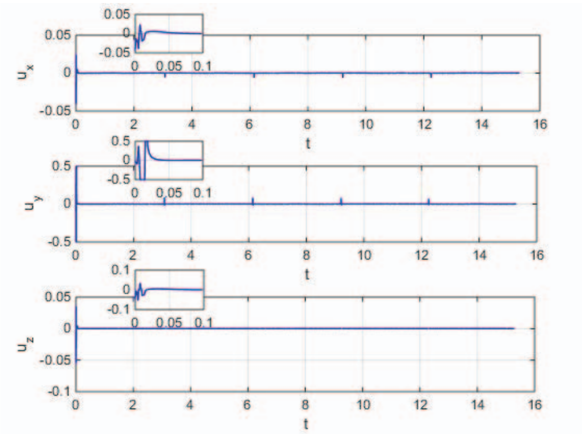

Fig. 6 Control acceleration

TABLE I. VELOCITY INCREMENT (m/s)

Items	*X-axis*	*Y-axis*	*Z-axis*	*Total*
5 periods	52.3583	364.4248	22.0595	368.8271
1st period	22.2206	299.3075	16.6149	300.5907
Average in 1 stable period	1.5862	3.4272	0.2866	3.7873

Through Fig.6, we can know that the control acceleration reaches its peak at the beginning, then declines to zero rapidly. Integrate the control acceleration and we can obtain the velocity increment required in the station-keeping control, which is presented in TABLE I.

Data in TABLE I show that the total velocity increment required during the 5-period simulation is $368.8271m/s$. Due to the initial errors added to the initial values, a much higher control acceleration is demanded at the beginning of the simulation, which leads to a huge velocity increment $300.5907m/s$ in the first period. When the simulation comes to its stable stage, the average velocity increment for a period is $3.7873m/s$, which is much lower than the first period. This shows that if the satellite can inject into the orbit more precisely, the control consumption in the beginning stage can be potentially reduced.

From the analysis of the simulation results, we can know that the station-keeping strategy proposed in this work is able to accomplish a relatively high precision. However, there is a trade-off between the precision and the control consumption, which means a higher precision requests a higher control consumption. What is more, a more precise reference orbit leads to a lower control consumption. In this work, the reference halo orbit is modified under CRTBP model, which isn't precise enough. Therefore, when modifying the reference orbit under a high fidelity model, the velocity increment required has the potential to decline in a large scale.

V. CONCLUSION

In this work, we firstly obtained the reference halo orbit based on the Richardson three-order analytic solution, differential correction and target shooting strategy under the CRTBP model. Then we designed a golden-section controller for velocity tracking and a PD controller for position tracking. Finally, we verified the controller through a simulation under ERTBP model. After analyzing the simulation results, we can conclude that the controller can accomplish a relatively high precision in station-keeping control of halo orbit; when the satellite comes to its stable stage, the control consumption demanded is pretty low. In future work, we will focus on the improvement of the precision of reference orbit to reduce the control consumption of the station-keeping control.

REFERENCES

[1] G. Gomez, J. Llibre, R. Martinez, C. Simo. Dynamics and Mission Design Near Libration Points, vol. 1. Singapore: World Scientific, 2001, pp.1-3.

[2] X. Y. Hou, L. Liu. "The dynamics and applications of the collinear libration points in deep space exploration," Journal of Astronautics, vol. 29, no. 3, pp.736-747, 2008.

[3] T. Zhou, D. Li, X. Chen, H. Yang. "Application of foreign spacecrafts of Sun-Earth libration points and manners of transfer trajectory," Missiles and Space Vehicles, vol. 5, pp.30-34,2004.

[4] R. W. Farquhar. "The control and use of libration-point satellites," Washington: NASA, 1970, pp.103-111.

[5] M. Shirobokov, S. Trofimov, M. Ovchinnikov. "Survey of station-keeping techniques for libration point orbits," Journal of Guidance, Control, and Dynamics, vol. 40, no. 5, pp. 1085-1105, 2017.

[6] K. C. Howell, H. J. Pernicka. "Station-keeping method for libration point trajectories," Journal of Guidance, Control, and Dynamics, vol. 16, no. 1, pp.151-159,1993.

[7] J. E. Kulkami, M. E. Campbell, G. E. Dullerud. "Stabilization of Spacecraft flight in halo orbits: an H_∞ approach," IEEE Transactions on Control Systems Technology, vol. 14, no. 3, pp.572-578, 2006.

[8] M. Xu, N. Zhou, J Wang. "Robust adaptive strategy for stationkeeping of halo orbit," Proceedings of 24th Chinese Control and Decision Conference, pp.3086-3091, 2012.

[9] M. Nazari, W. Anthony, E. A. Butcher. "Continuous thrust stationkeeping in Earth-Moon L1 halo orbits based on LQR control and Floquet theory," AIAA/AAS Astrodynamics Specialist Conference, pp.1-18,2014.

[10] H. X. Wu, J. Hu, Y. C. XIE. Characteristic model-based intelligent adaptive control, Beijing: China Science and Technology Press, pp.1-2, 2009.

[11] P. Gurfil, D. Meltzer. "Stationkeeping on unstable orbits: generalization to the elliptic restricted three-body problem," The Journal of the Astronautical Sciences, vol. 54, no. 1, pp.1-23, 2006.

[12] Y. Meng, Y. Zhang, Q. Chen. Dynamics and control of spacecraft near libration points, Beijing: Science Press, pp.1-2, 2015.

[13] D. L. Richardson. "Analytic construction of periodic orbits about the collinear points," Celestial Mechanics, vol.22, pp.241-253, 1980.

[14] M. Popescu, V. Cardos. "The domain of initial conditions for the class of three-dimensional halo periodic orbits,". Acta Astronautica, vol. 36, no. 4, pp.193-196. 1995.